UNFOCUSED SOURCE OF X-RAYS IN A MICROFOCUS X-RAY TUBE

W.D. Friedman

BP America
4440 Warrensville Center Road
Cleveland, OH 44128

INTRODUCTION

In an ideal microfocus X-ray tube all the radiation would emanate from a single point, typically 10μm or less in diameter. The intensity would also be independent of angle within the cone beam that is defined by apertures within the tube. Such a tube would have high resolution due to the small spot size, and the uniform distribution of X-ray photons on the detector plane would make it useful for measuring density variations in flat samples such as ceramic modulus of rupture (MOR) bend test bars. Koenigsberg and Cotter [1] have shown that there are additional sources of X-rays in microfocus tubes that create anomalous shadows in images of MOR bars, making it difficult to assess their uniformity. They demonstrated that the secondary sources can be eliminated by placing a tungsten aperture in the tube [2]. While this cured the problem of anomalous shadows, it did not determine the cause of the secondary source. In this work, a pinhole camera is used to determine the shape and size of the secondary sources, enabling the structures that scattered the primary X-rays to be identified.

THE SHADOW ANOMALY

If an X-ray tube emits a cone of X-rays from a single focal spot, then Figure 1 shows that the intensity of these primary X-rays produces a shadow of the object which has a uniform intensity. At the edge of the object there is a gradation in intensity due to the oblique X-rays penetrating different thicknesses at the edge of the object, but this is not the cause of the shadow anomaly and is not depicted in Fig. 1. However, if there are additional sources of X-rays outside the primary focal spot, these secondary X-rays will have direct paths to regions of the detector that fall within the shadow of the primary source. Since these X-rays do not pass through any of the material in the object, even relatively weak secondary sources can have a noticeable effect. This additional intensity is seen as increased density on film, thus it is known as anomalous shadowing. In Fig. 1 these sources are assumed to be in the shape of rings surrounding the primary focal spot and are considered to be unfocused since they are not point sources. The width of the emitting region will cause a blurring of the edge of the shadow in the image, which is shown as a gradation of

Review of Progress in Quantitative Nondestructive Evaluation, Vol. 11
Edited by D.O. Thompson and D.E. Chimenti, Plenum Press, New York, 1992

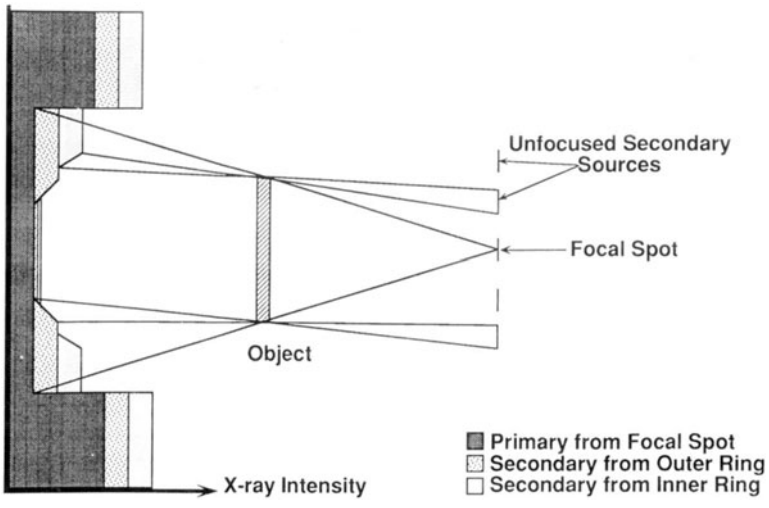

Figure 1 Distribution of X-ray intensity at the detector plane due to multiple sources in a microfocus X-ray tube. The secondary sources can create anomalous shadows near the edge of the object.

intensity in Fig. 1. Circular sources would also explain why the anomalous shadows are parallel to the edge of objects, independent of the objects orientation.

EXPERIMENTAL TECHNIQUES

The best method for imaging a source of X-rays is a pinhole camera. It is easy to implement and the spatial resolution can be controlled by choosing a pinhole diameter that is approximately equal to the desired resolution. Pinhole cameras with small apertures can be difficult to align due to the low flux passing through the hole. Since the goal is not to measure the structure of the primary focal spot, a large pinhole can be used to image the location and shape of the secondary sources as shown in Figure 2. In this schematic view X-rays are shown emanating from the 10μm focal spot of a microfocus X-ray tube [3]. The primary X-rays pass through the 1.1μm hole drilled in a 0.75mm lead sheet, but are intercepted by a 0.75mm thick beam block so they do not overexpose the image intensifier. X-rays that are scattered from structures within the X-ray tube become the unfocused secondary sources and are imaged by the pinhole if they are outside the cone angle obscured by the beam block. The resolution and field of view of the camera determine the choices for the diameter of the pinhole and beam block, and their placement. Due to the structure of the X-ray tube, the secondary sources are expected to be within a 2 cm circle. A camera magnification of 4 will make it easy to center this region within the 22 cm diameter of the image intensifier. Based on similar triangles, the ratio of distances to the pinhole determines the magnification. Thus a tube to pinhole distance of 14 cm and a tube to image plane distance of 68 cm produce a magnification of (68-14)/14 = 3.85. Resolution is computed by determining the size of the pinhole shadow produced by a point source at the image plane, and then computing its corresponding size at the source plane. The

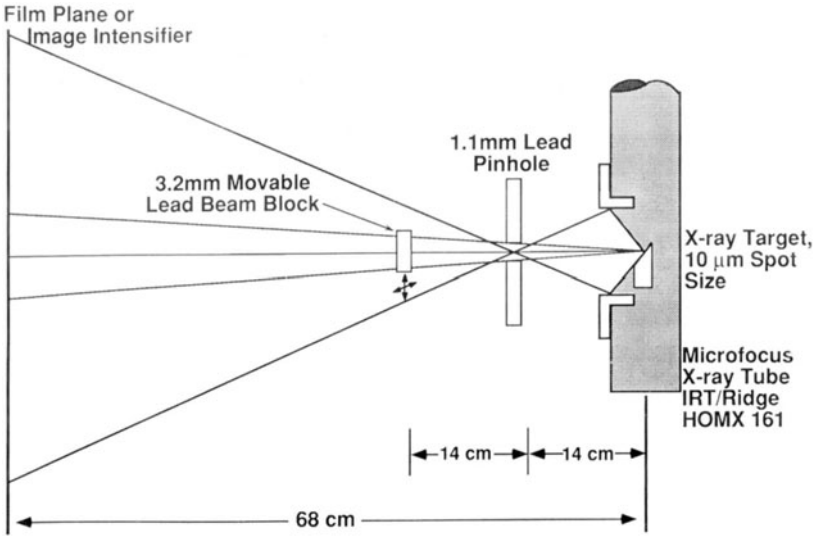

Figure 2 A large aperture pinhole camera used to image the position of unfocused secondary X-ray sources represented here by X-rays scattered from an aperture at the front of a microfocus X-ray tube.

point source projects the pinhole size as 68/14 x 1.1 = 5.3mm at the image plane. Dividing by a camera magnification of 3.85 yields an equivalent source size of 1.4 mm at the tube plane. Thus an object in the tube plane must be blurred by that amount. The beam block is positioned the same distance from the pinhole as the X-ray tube, thus for primary X-rays its magnification will be 1/2 that of the pinhole. It needs to be at least twice the pinhole diameter to block the primary X-rays, three times is chosen to simplify the alignment. When imaged by the pinhole, the beam block's magnification is the same as objects in the plane of the X-ray tube, thus it will obscure a 3.2mm diameter circle centered around the primary source. The field of view at the tube plane for secondary sources will then be between 3.2 and 57mm with the image intensifier as the detector, and can be larger if the image is recorded on X-ray film that is larger than 22 cm.

The beam block disk is cut with a punch from a 0.75mm thick sheet of lead. It is suspended on clear plastic adhesive tape stretched across a 7.5cm diameter ring that is attached to the x-y-z sample stage of the real time system. The 1.1mm pinhole is drilled in 0.75mm lead and is mounted on a 3mm lead sheet that is suspended from an optical mount attached to the X-ray tube with hose clamps. The camera is aligned with the real time system using 30 keV X-rays to avoid saturating the TV camera or the image intensifier. The alignment is done by first centering the image of the beam block on the intensifier. The pinhole is then moved iteratively by turning off the X-rays until its image is near the marked position of the beam block. The calibrated motor drives on the x-y stage now translate the beam block until it obscures the direct beam through the pinhole. The X-ray

energy can now be increased until there is sufficient transmitted flux through the lead to accurately center the image of the pinhole on the beam block.

EXPERIMENTAL RESULTS

Two photographs of the real time TV monitor are shown in Figure 3 with the display contrast adjusted to show particular features. In these images white represents increased X-ray intensity. The left side emphasizes the image formed by the primary X-rays of the beam block with the pinhole centered on it. On the right side are seen ring and horseshoe shaped unfocused secondary sources. The background white area is due to the transmission of primary X-rays through the 0.75mm lead substrate in which the pinhole is drilled. The dark region on the bottom is the outline of a 3mm thick lead plate that supports the pinhole substrate. The size of the features is determined by calibrating a video caliper with the 12.7mm opening in the 3mm lead plate in the plane of the pinhole and then applying a correction factor for the magnification of 68/(68-14) so that the read out is in terms of distances in the plane of the X-ray tube. However, this calibration is only correct for images formed by secondary X-rays passing through the pinhole. Figure 4 is taken under the same X-ray conditions, except the image is recorded on X-ray film in a 20 minute exposure. Because of the larger dynamic range, there is an additional dark circle surrounding the beam block image. The three smaller circles in the center of the image are identified in Figure 5. Each of these circles has a different magnification. The magnification of the direct image of the pinhole is 68/14 = 4.85, while that for the primary illuminated direct image of the beam block is 68/28 = 2.43, while the pinhole imaged beam block using unfocused secondary X-rays is (68-14)/14 = 3.85. The images formed by the direct X-ray beam from the 10μm focal spot have sharp edges, while those formed by the pinhole are broadened. With a broad source the image edges will be blurred, as is seen for the larger image of the beam block.

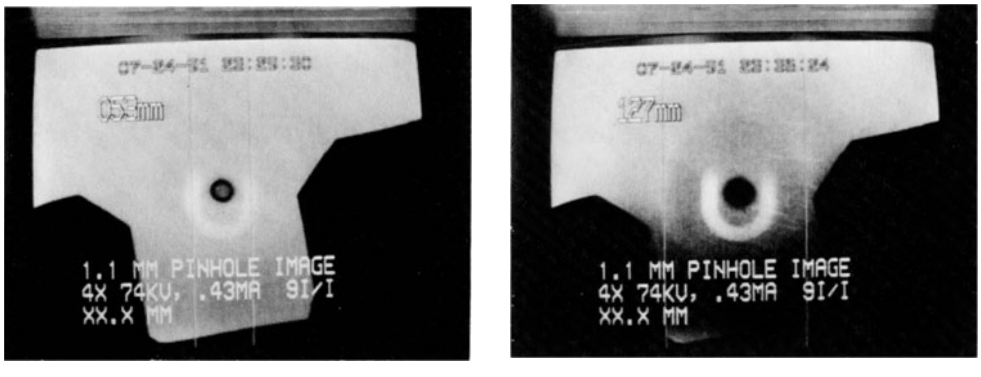

Figure 3 Pinhole images of unfocused secondary sources photographed from the TV monitor of a real time X-ray system using an image processor to produce different contrast settings. The vertical cursor lines delineate the horseshoe and ring shaped secondary sources.

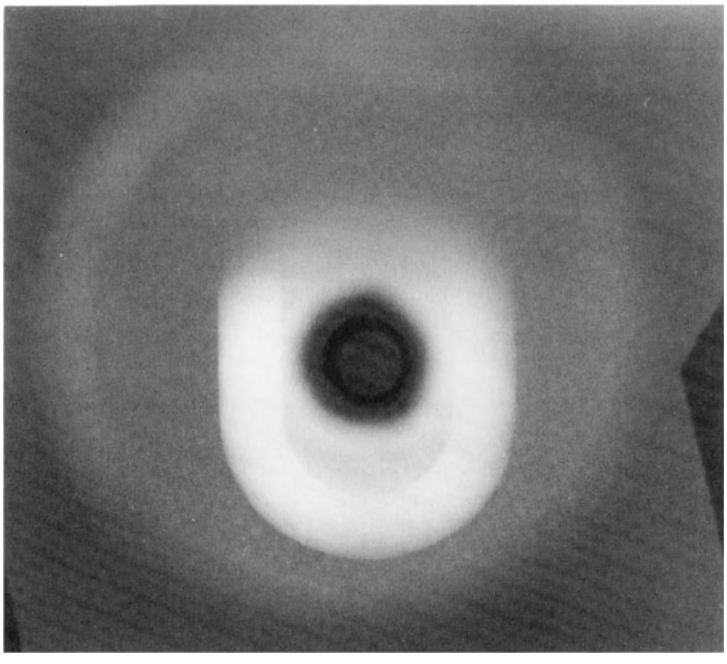

Figure 4 Pinhole image recorded on Kodak Industrex B X-ray film and printed as a low contrast positive image to retain a large dynamic range. Conditions are 74 kV, 0.43 mA, 20 minute exposure, and development in a medical film processor. White represents increased X-ray intensity.

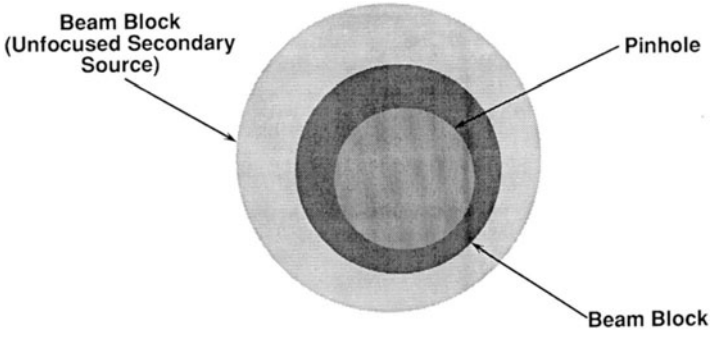

Figure 5 Identification of the features being imaged within the horseshoe shaped region in Figure 4. The inner two circles with sharp edges are the images of the pinhole and the beam block formed by primary X-rays which pass through the 0.75mm lead of the beam block and pinhole substrate. The larger diffuse image is the shadow of the beam block formed by unfocused secondary X-rays which pass through the pinhole directly to the film without any attenuation.

DISCUSSION OF RESULTS

The real time and film images of Figures 3 and 4, respectively, demonstrate that there are two regions outside the primary focal spot that are sources of X-rays. The use of a beam block allows them to be seen in real time. The large circular region has an apparent diameter in the tube plane of 12.7 mm and the smaller horseshoe shaped region is 5.3 mm across. Figure 6 shows the interior structure of the X-ray tube and the objects that could possibly scatter primary X-rays and thus become unfocused secondary sources. Koenigsberg and Cotter added an additional tungsten collimator inside the tube and an external lead collimator, which eliminated the anomalous shadows they had seen. The placement of the collimators mainly prevents primary X-rays from striking the edge of the aluminum bushing which has an inner diameter of 11mm. Since our tube does not have this additional collimation, scatter from this bushing must correspond to the 12.7mm ring seen with the pinhole camera. The size difference is explained by the edge of the bushing being imaged with a larger magnification since it is closer to the pinhole than it is to the centerline of the X-ray tube, which the video caliper is calibrated to. The spreading of the circular line in the image is consistent with the size of the pinhole. The circular shape of this source also explains why the anomalous shadows were always parallel to an edge no matter what the orientation of the edge.

The horseshoe shaped region is generated by the edge of the brass target stop, shown in Figure 7, that is butted against the top of the X-ray target to hold it at the correct

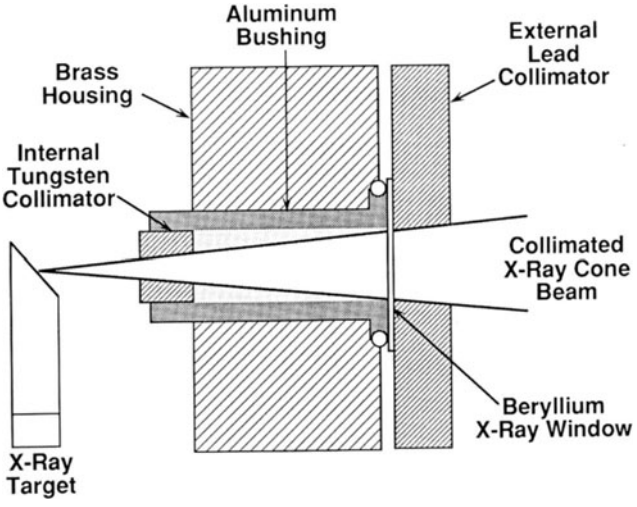

Figure 6 Internal structure of the microfocus X-ray tube. Placement of the tungsten and lead collimators added by Koenigsberg and Cotter to eliminate the effect of secondary X-ray sources is shown, but they were not in the tube used for these measurements.

distance for the electrons to focus on it. The "U" is formed by scattering from the edge of the slot milled into the end of the target stop to let the primary X-rays pass from the target to the beryllium window. The pinhole camera inverts the image so the arch of the U is at the bottom. The effect of this source could be reduced by making the U shaped opening larger than the field of view of the collimators.

The film based image of Figure 4 also shows a weaker emitting region inside the U that must correspond to the target surface outside the focal spot. Without this secondary source there would not be the second larger and blurred image of the beam block. The cause of this large area source is not known, potential candidates are unfocused but accelerated electrons, or some scatter of focused electrons incident on the target.

A comparison of the X-ray flux from the primary focal spot and the secondary sources was made by calibrating the film response at 40kV and using it to convert the measured film density in those regions to X-ray intensity. The available energy was estimated by multiplying this intensity by the apparent emitting area. In arbitrary units the ratios are:

primary focal spot	outer ring	horseshoe
1000	9	6

If the secondary sources are not removed by internal collimation then they can illuminate regions near an edge that are in the shadow of the primary focal spot. Supposing an object thickness which attenuates the primary X-rays by a factor of 10, then the ratio of secondary to primary X-rays could be $(9+6)/(1000\div10) \sim 0.15$. This would be sufficient intensity to produce the anomalous shadows seen by Koenigsberg and Cotter.

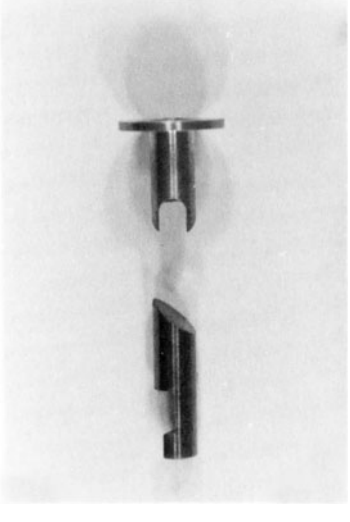

Figure 7 Tungsten anode with target surface cut at an angle and the brass target stop which locates the anode at the correct distance for the electron beam to focus on.

CONCLUSIONS

The pinhole images have demonstrated that the anomalous shadows are caused by two sources of secondary X-rays. These sources are caused by scattering of primary X-rays from the edges of objects inside the microfocus tube. The entire tungsten target also appears to be a weak diffuse source of X-rays. It is recommended that manufacturers of X-ray tubes pay more attention to this problem and eliminate the edges or incorporate additional internal collimators. While the secondary sources have been imaged in real time when the primary source is obscured with a beam block, the anomalous shadows have not been observed in real time images even when the contrast has been enhanced electronically. One reason these shadows are not seen in real time images is due to the limited dynamic range of some video detectors. To avoid saturating the TV camera it is common practice to arrange lead shutters near the edge of the object being radiographed to prevent direct primary X-rays from reaching the camera. These beam blocks could also obscure the X-rays from the unfocused secondary sources that cause the anomalous shadows. The use of CCD cameras, which tolerate overexposure, might allow these shadows to be observed on real time systems.

ACKNOWLEDGEMENTS

The author would like to thank W. D. Koenigsberg of GTE for the kind permission to use the illustration showing the method for curing the shadow artifact with an internal aperture.

REFERENCES

1. W. D. Koenigsberg and D. J. Cotter, "On the Origin of Anomalous Shadows in Microfocus Projection Radiography," Conference on Nondestructive Evaluation of Modern Ceramics, (The American Society for Nondestructive Testing, Columbus, 1990) p.56.

2. U.S. patent 5033074.

3. HOMX 161 manufactured by Ridge (Tucker, Georgia) now IRT Corporation; (San Diego, CA).